ASYMMETRICAL SQUARAINE SENSITIZERS WITH VARYING Π-BRIDGES AND ANCHORING GROUPS FOR DYE SENSITIZED SOLAR CELLS

A Thesis
Presented to
The Academic Faculty

by

Gabriel Pajares

In Partial Fulfillment
of the Requirements for the Degree
Bachelor's of Science with the Research Option in the
School of School of Chemistry and Biochemistry

Georgia Institute of Technology
May 2015

ASYMMETRICAL SQUARAINE SENSITIZERS WITH VARYING Π- BRIDGES AND ANCHORING GROUPS FOR DYE SENSITIZED SOLAR CELLS

Approved by:

Dr. Seth Marder, Advisor
School of Chemistry and Biochemistry
Georgia Institute of Technology

Dr. Dong Qin
School of Material Science and Engineering
Georgia Institute of Technology

Date Approved: ___4/30/2015_____

Para mi viejo que me enseño a mirar el mundo como un estudiante.

ACKNOWLEDGEMENTS

I wish to thank Fadi M. Jradi for his patience and kindness in personally guiding me through each of the challenges posed by our project. I want to thank Mostafa El-Sayed and his group for their significant collaborations on this project, they conducted the photovoltaic measurements and fabricated the cells used in our analysis. I also wish to thank Dr. Marder for the advice that permeated through the walls of his laboratory and into my everyday life, my goals, and dreams. Lastly, I want to thank my fiancée, Elizabeth Deaver, for her love, grace, and for saying yes to the most important question of my life.

TABLE OF CONTENTS

		Page
ACKNOWLEDGEMENTS		iv
LIST OF TABLES		vi
LIST OF FIGURES AND SCHEMES		vii
SUMMARY		viii
CHAPTER		
1	Introduction	1
2	Materials	8
	Synthesis of Indoles with Out-of-Plane, Bulky Cycloalkanes	8
	Synthesis of Asymmetric Squaraine Bromide	12
	Synthesis of Thiophene Bridge with Perfluorinated Alkyl Chain	18
3	Optoelectronic Properties and Effects of Aggregation	22
4	Measurements of Photovoltaics	28
5	Conclusion	31
REFERENCES		33

LIST OF TABLES

Page

Table 1: Optical properties and electrochemical properties of the synthesized dyes 22

Table 2: Charge injection dynamics of YR6, TS3, and other CA and PA series. 25

Table 3: Measurements of photovoltaics using optimized CDCA:Dye ratios 28

LIST OF FIGURES AND SCHEMES

FIGURES

Page

Figure 1: Absorption spectra of a squaraine dye in ethanol and on 2.8 μm TiO_2 film 3

Figure 2: Chosen cycloalkane groups shown representatively on the squaraine 4

Figure 3: Molecular structures comparison of typical indole against proposed group 4

Figure 4: Proposed squaraines with varying π-bridges and acceptor groups 5

Figure 5: Chemical structure of **GMPII** containing perfluorinated alkyl chains 6

Figure 6: Proposed bulking groups for future integration into squaraine dye 8

Figure 7: Target squaraine dyes with cycloalkanes **GMPIII** and **GMPIV** incorporated 9

Figure 8: UV-vis absorption spectra of all dyes measured in ethanol 24

Figure 9: UV-vis absorption spectra of all dyes after application on TiO_2 films 26

Figure 10: Photovoltaic performance of all dye cells in TiO_2 films 29

Figure 11: Measured IPCE of the optimized dye cells with dye bathed TiO_2 films 30

SCHEMES

Scheme 1: **GMPVII** and **GMPVIII** were used in order to prepare **GMPIX** 12

Scheme 2: Overview of the synthetic route taken to produce the **GMPII** 18

Scheme 3: Alternate pathway for the synthesis of **GMPII** 19

SUMMARY

The work detailed below is a product of three different synthetic projects throughout three semesters in the Marder lab. The first project dealt with the synthesis of a squaraine bromide sensitizer for further use in PhD candidate, Fadi Jradi's work. His work explored the effect of introducing conjugated π-bridges equipped with different solubilizing groups, and anchoring groups on the overall performance of asymmetrical squaraines; namely by enhancing their high energy absorption, reducing dye aggregation as well as electron recombination from the mesoporous TiO_2 into the acceptors in the electrolyte. The second project looked into the effect of molecular iodine, a species that can be generated locally near the TiO_2 surface,[1] on enhancing unwanted electron recombination from TiO_2 into the electrolyte. The synthesis of a squaraine-based dye containing a long, fluorinated alkyl chain, which have low binding affinity to iodine, positioned near the TiO_2 surface can create a pseudo blocking layer which prevents acceptors in the electrolyte, namely molecular iodine, from capturing an injected electron from TiO_2. The third project consisted of the incorporation of large, out-of-plane cyclic groups in the indole region of a donor- π-acceptor dye with the goal of studying the modification's effect on dye spacing, aggregation, and possible excited state quenching.

The latter two projects were not able to be completed, yet some understanding of synthetic steps and procedures was gained. Therefore, the focus of this thesis was placed mainly on the incorporation of different π-bridges including thiophene (T), 4-hexyl-4H-dithienopyrrole (DTP), dithieno[3,2-b:2',3'-d]thiophene (DTT), and 4,4-bis(2-ethylhexyl)-4H-silolo[3,2-b:4,5-b']dithiophene (DTS) along with varying anchoring groups cyanoacetic acid (CA) and cyanophosphonic acid (PA) into the squaraines'

chemical structure and how each of these modifications affected solar cell performance. In summary, it was found that dyes with DTS bridges had the highest measured power conversion efficiencies in their respective groups at 8.9% for the CA series and 5.0% for the dye with the PA anchoring group. These properties were attributed to the higher short circuit currents (*Jsc*) and open circuit voltages (*Voc*) from the decreased dye aggregation and slower recombination rates, respectively. The study suggests dye aggregation can be potentially decreased by incorporation of out-of-plane π-bridge groups with respect to the planar squaraine molecule used. This was seen in the increased *Jsc* and subsequently in the increased power conversion efficiencies (PCE).

CHAPTER 1

INTRODUCTION

The discovery of the photovoltaic effect by French physicist Edmond Becquerel in 1839, [2] described a phenomenon in which the presence of light is able to trigger an electric voltage between two electrodes in a system. In essence, the principle of harvesting solar energy in the form of electric potential has proven revolutionary as it has provided a gateway into an energy source with the largest potential to fulfill the world's future energy needs. [3] In the past century alone, the increase in global demand of energy as well as increasing pollution, global warming, and the search for safe, renewable energy has triggered a cascade of research into the evolution of a device that could efficiently apply the conversion of solar energy into a voltage of useful quantities.[4] D. M. Chapin introduced the first silicon solar cell in 1954,[5] since then, and due to subsequent enhancements in the solar cell engineering, along with the development of new materials, solar cells continue to change as new types are fabricated.

Focusing on a potentially promising type of solar cells, dye sensitized solar cells (DSSCs) offer several advantages over other photovoltaic devices such as low production costs and ease of fabrication.[6] The cell itself is composed of three major components- a sensitizer, redox shuttle/electrolyte, and photoanode consisting of mesoporous titania. Generally in DSSCs, light is absorbed by a sensitizer dye bound to mesoporous TiO_2. Upon photoexcitation of the sensitizer, the excited electron is rapidly injected into the TiO_2 where it diffuses through the semiconductor and is eventually collected to do work. DSSCs are characterized by a quick, regenerative photochemical process as the oxidized sensitizer is regenerated by an electrolyte such as iodide/triiodide (I_3^-/I^-) dissolved in solution.[7]

Varying types of sensitizers have been incorporated into DSSCs including ruthenium based dyes, and organic based dyes such as porphyrin,[8] and squaraine dyes.[1] Ruthenium based dyes exhibit a broad absorption spectrum, suitable excited and ground state energy levels, and significant electrochemical stability. However, ruthenium based dyes lack high molar absorptivity and therefore a large amount of adsorbed dyes are required in order to collect light efficiently. Dyes with higher molar absorptivity coefficients, such as squaraine sensitizers, can be manufactured on thinner TiO_2 films. This reduces the electron diffusion distance and hence decreases the probability of an electron being intercepted by the electrolyte.[1]

Squaraine sensitizers, exhibit strong extinction coefficients and absorb strongly in the near infrared region around 650 nm. Unlike the most commonly used dyes, such as porphyrin based dyes which lack the ability to significantly absorb in the near infrared region, squaraines have the potential to become panchromatic absorbers with appropriate engineering. This quality would allow for absorption of all light in the solar spectrum, from 920 nm to 400 nm, which is needed for optimal light harvesting, rendering squaraines interesting to study in DSSCs. Three parasitic processes, however, can limit the operation of DSSCs including (1) the decay of the excited dye before it is able to inject its electron into mesoporous TiO_2, (2) recombination of the injected electron with the oxidized dye before it is reduced, and lastly (3) the I_3^-/I^- redox shuttle can intercept the injected electron from the semiconductor before it is collected.[1] The rapid injection of electrons from the excited dyes into TiO_2 (femtosecond timescale), renders the first parasitic process unlikely. However, the planar structure of this class of dyes has been previously shown to prompt dye aggregation on surfaces such as mesoporous TiO_2 (**Figure 1**).[9] The tendency for squaraine dyes to strongly aggregate decreases the distance between the dye molecules and thus increases the probability of excited state quenching by a nearby cation, as opposed to electron injection into TiO_2, required for optimal performance. Molecular iodine, which is usually not present in the electrolyte due to the

high iodide concentration, can in fact proliferate near the TiO_2 surface, depending on the dye's chemical structure. For example, the presence of good σ-donors,[10] such as sulfur atoms commonly used in the bridging units of sensitizers,[11] favor the formation of unwanted molecular iodine which has been shown increases the probability of charge recombination.[12]

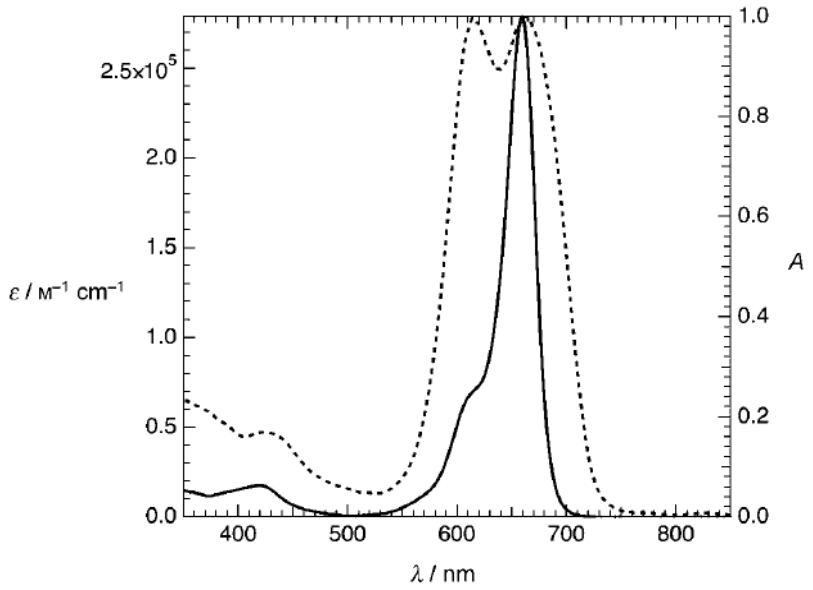

Figure 1. Absorption spectra of a squaraine dye in ethanol (solid line) and on a 2.8 μm TiO_2 film (dotted line). The aggregate peak appears blue shifted from the squaraine peak at around 600 nm.

The first project proposed structural modification of an unsymmetrical squaraine-based dye **GMPI** (**Figure 2**), namely by bulking up the indole-derived groups in order to study the effects of these groups on dye-dye aggregation. Due to the planar structure of squaraine based dyes, aggregation becomes a significant problem leading to decreases in the J_{sc} of the cell (**Figure 3**). Despite their prior partial success, straight, unbranched alkyl chains were not chosen for this project, due to higher degrees of freedom available within their structures.[13] Instead, we aimed on incorporating midsized cycloalkanes, whose larger volumes and relatively restrained structures, are expected to enhance dye spacing.

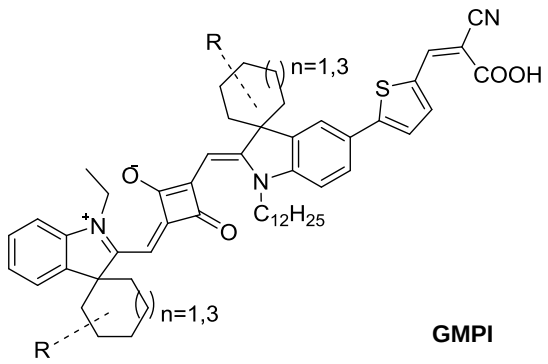

Figure 2. Chosen cycloalkane groups shown representatively on the squaraine based dye.

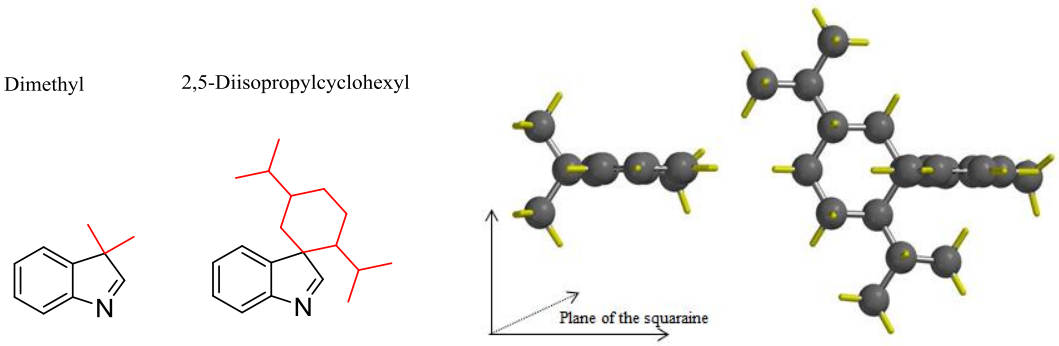

Figure 3. *Left:* Molecular structure of typical indole groups displaying the standard dimethyl groups versus one of the proposed cycloalkanes (red). *Right:* Modeling of the dimethyl substituted indole group vs. one of the proposed cycloalkanes.

During the second project, focus was directed towards extending the absorption of a set of squaraine dyes into the 450-550 nm region while also including different spatial arrangements of solubilizing groups that can reduce aggregation. Eight squaraine dyes with T, DTP, DTT, and DTS π-bridges with CA and PA acceptor/anchoring groups were synthesized for the purpose of this project (**Figure 4**).

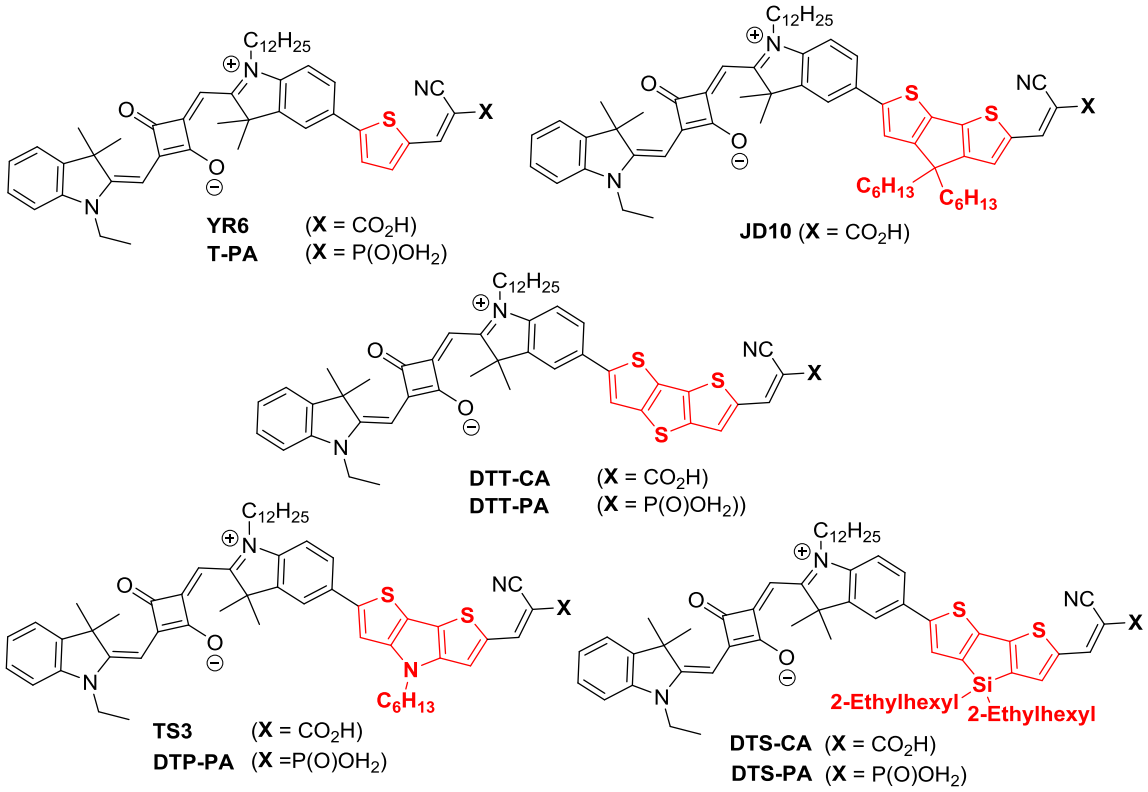

.

Figure. 4. Proposed squaraines with varying π-bridges and acceptor groups. Molecular structures of the squaraine dyes proposed. **YR6**, [9] and **JD10**, [14] have been reported previously and used in this document strictly for comparison.

These dyes served to further study the effects of varying π-bridges which possess high energy absorption bands complimentary to the near-infrared (NIR) absorption region of the squaraine. The extended conjugation provided by these bridges also shifted the absorption band of the squaraine towards longer wavelengths, thereby increasing its panchromaticity. This holds the potential to increase its incident photon to current efficiency (IPCE) if efficient electron injection is maintained. [15]

It is also important to note the effects of anchoring groups within the eight dyes synthesized. CAs are known for their stability and relative ease of incorporation into a sensitizer. Furthermore, these anchoring groups have been shown to outperform other analogs used for the same purpose via their higher J_{sc}.[16, 17, 18] The study found that while

the injection efficiency of CA dyes was better than PA, electron recombination was higher with CA dyes than PA dyes. Furthermore, the reasons behind their increased J_{sc} are not yet completely understood due to a multitude of factors. This includes higher surface coverage of CA based dyes due to an upright conformation on the substrate increasing the number of dye molecules bound to the surface.[16] PA dyes showed higher device stability, compared to CA, especially after 1000 hours of light soaking,[18] due to their much higher binding constants to TiO_2.

In the third project, the proposed low molecular iodine binding affinity groups, perfluorinated alkyl chains, were chosen to be incorporated into the thiophene bridge of a squaraine sensitizer, **GMPII** (**Figure 5**). Therefore, the project first dealt with determining the best synthetic route in terms of ease and percent yield for the target compound.

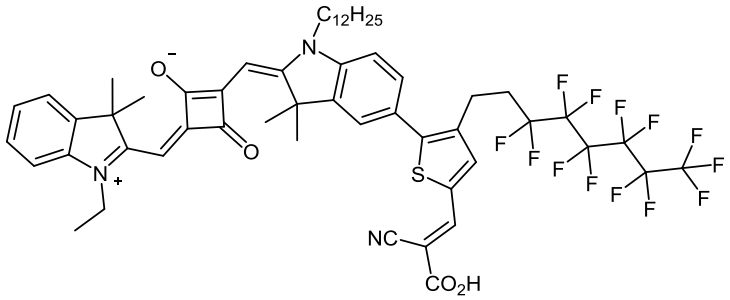

GMPII

Figure 5. Chemical structure of **GMPII** containing perfluorated alkyl chains.

If successful, **GMPII** would potentially provide information about the effect of reducing dye-electrolyte interactions in generating molecular iodine near the surface along on charge recombination, electron lifetime, and ultimately on the V_{oc} of the cell.

Increases in the solar cell V_{oc} can be translated to an increase in solar to electric power conversion efficiency, PCE, according to:

$$\text{PCE} = (J_{sc} \times V_{oc} \times FF) / P_{in}$$

where *FF* the fill factor, and P_{in} the total solar power incident on the cell.

In this document, an approach to studying the effects of electrolyte charge recombination is presented along with two different approaches for combating aggregation of planar squaraine sensitizers. One project focusing on aggregation yielded sensitizers for application into solar cell allowing for measurements of their optoelectronic and photovoltaic properties along with aggregation effects, ultimately producing data on PCE.

CHAPTER 2

MATERIALS

Synthesis of Indoles with Out-of-Plane, Bulky Cycloalkanes

An approach to decreasing aggregation was pursued focusing on bulking up the indole groups of a symmetrical squaraine dye. We aimed on incorporating midsized cycloalkanes, **GMPVI** and **GMPVII** shown in **Figure 6**, whose larger volumes, relatively restrained structures, and out-of-plane conformation with respect to the planar squaraine were expected to enhance dye spacing.

GMPIII **GMPIV**

Figure 6. Proposed bulking groups that will be integrated into the indole-derived region of an unsymmetrical squaraine dye.

The structures shown above would first be synthesized separately from the squaraine and later incorporated into the indole region as yielding **GMPV** and **GMPVI** as shown in **Figure 7**.

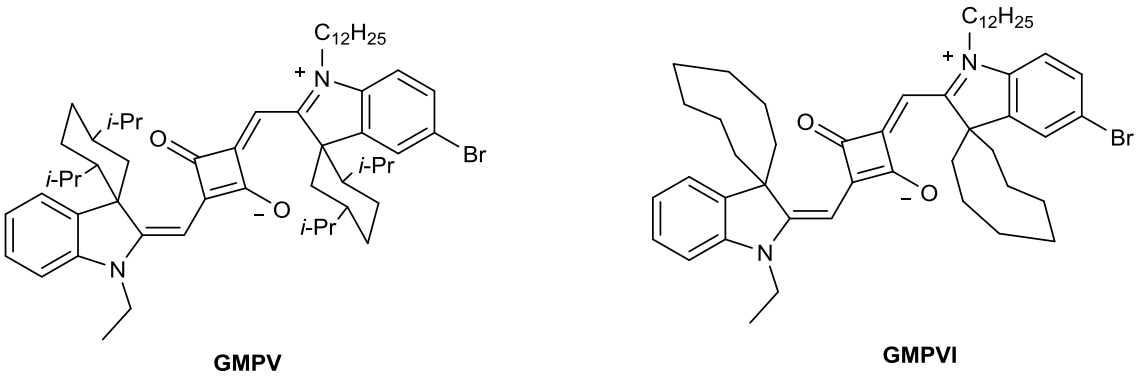

Figure. 7: Target squaraine dyes with cycloalkanes **GMPIII** and **GMPIV** incorporated respectively.

5-(methoxymethylene)-1,1,3,3-tetramethylcyclohexane (2a): Dry sodium hydride (600 mg, 25.92 mmol) was added into a dry 50 mL round bottom flask. (methoxymethyl)triphenylphosphonium chloride (2.73 g, 7.97 mmol) dissolved in dry tetrahydrofuran (30 mL) was then introduced to the flask under a nitrogen atmosphere. The suspension was then cooled to 0 °C. The reaction was then warmed to room temperature and stirred for 6 hours. 3,3,5,5-tetramethylcyclohexan-1-one (**1a**) (1.00 mL, 6.48 mmol) was then added and the reaction was refluxed overnight at 86 ^{o}C. The following reaction mixture was extracted in ether (4 x 10 mL) and product, **2a**, was noted as a peak in the GCMS at 60% conversion.

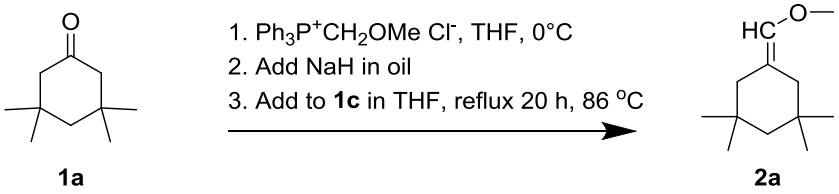

1-cyclooctylethan-1-ol (4a): **3a** (16.6 g, 148 mmol), ethanol (15.8 g, 343mmol) and mercury (1.00 g, 4.98 mmol) were introduced into a 250 mL quartz round bottom flask.

The round bottom flask was purged with N_2 for 15 minutes and introduced into the photo-reactor overnight and under 256 nm exposure. The reaction mixture was removed and was concentrated under pressure. The concentrate was run through a silica gel column packed and run in hexanes to elute only the starting material. The rest of the column was moved using a gradient of 50% - 100% ethyl ether in hexanes. **4a** (1.76 g, 6%).

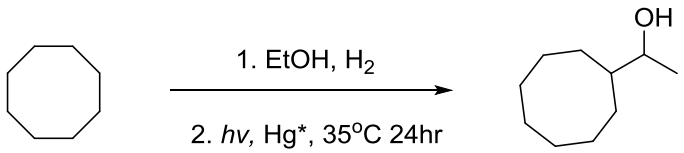

3a **4a**

1-cyclooctylethan-1-one (5a): Potassium permanganate (11.13 g, 70.49 mmol) and copper sultfate pentahydrate (11.10 g, 44.46 mmol) were ground into a fine dust and introduced into a 250 mL round bottom flask along with benzene (30 mL). **4a** (1.70 g, 10.87 mmol) was added followed by stirring for two nights at room temperature. The oxidant powder mixture was removed by vacuum filtration while washing with benzene. Filtrate was concentrated followed by a silica gel column was packed and eluted with dichloromethane producing three fractions, checking their identity using $KMnO_4$ staining of TLC plates. Product, **5a**, was identified via GCMS at 44% conversion (0.74 g)**.**

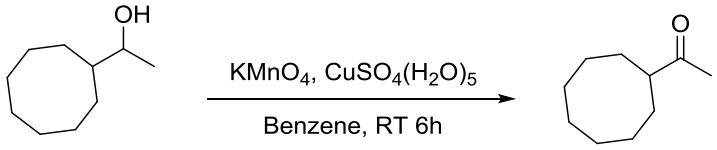

4a **5a**

5'-bromo-2'-methylspiro[cyclooctane-1,3'-indole] (6a): (4-bromophenyl)hydrazine hydrochloride (0.43 g, 1.94 mmol) was dissolved in ethanol (5 mL) and refluxed under

nitrogen for 3 hours and monitored by thin layer chromatography. The ethanol was evaporated under reduced pressure and acetic acid (6.5 mL) was added into the reaction mixture and refluxed under nitrogen overnight. A saturated sodium bicarbonate solution (40 mL) was added to the reaction mixture and once the fizzing stopped, dichloromethane (3 x15 mL) was used to extract the organic layer which was purified by a silica gel column using dichloromethane as an eluent to get **6a**. Product was identified via GCMS at 32% conversion (0.19 g).

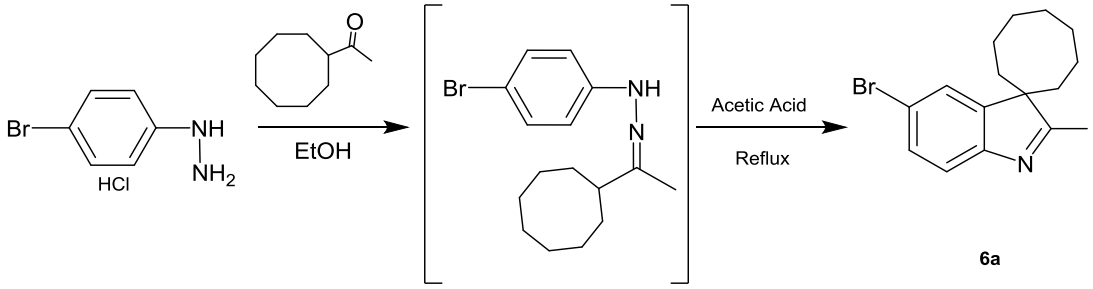

Synthesis of Asymmetrical Squaraine Bromide

The common squaraine donor intermediate, **GMPIX**, was prepared following the published reaction pathway reported by Shi et al. as shown in **Scheme 1**.[9]

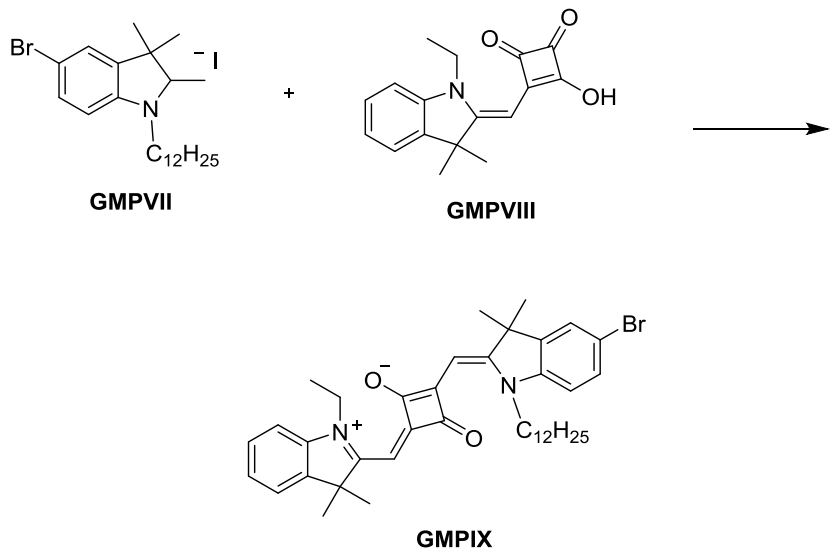

Scheme 1. **GMPVII** and **GMPVIII** were used in order to prepare **GMPIX** as described below.

The synthesis of the asymmetrical squaraine took place using two different pathways ultimately combining **GMPVII** and **GMPVIII** to form **GMPIX**.

5-bromo-2,3,3-trimethyl-3H-indole (2b): **1b** (1.25 g, 6.7 mmol) and 3- methyl-2-butanone (1.15 g, 13.4 mmol) were refluxed in ethanol (15 mL) under a nitrogen atmosphere for 30 minutes. Acetic acid (15 mL) was then added and the reflux continued during the next three days. The reaction mixture was then poured over a saturated sodium bicarbonate solution (100 mL) and the organic layer extracted by dichloromethane (95 mL), dried with anhydrous sodium sulfate and concentrated producing a red oil, **2b**, (1.48 g, 93%) which was used in the next step without further purification

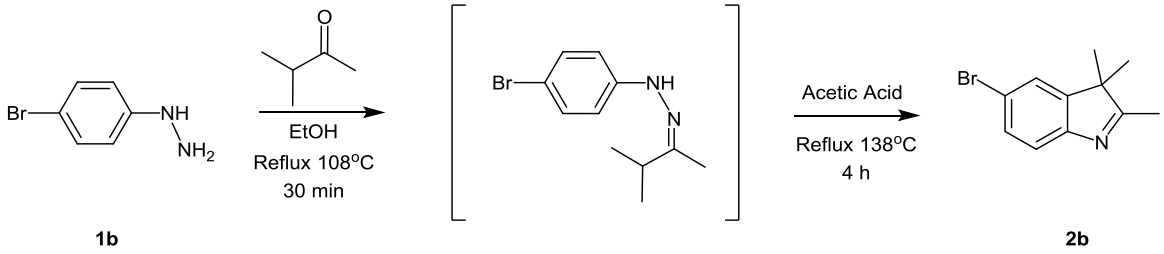

5-bromo-1-dodecyl-2,3,3-trimethyl-3H-indol-1-ium iodide (GMPIII): **2b** (1.47 g, 6.2 mmol) and 1-iododecane (14.70 g, 50 mmol), were dissolved in acetonitrile (10 mL) and refluxed under a nitrogen atmosphere overnight. The reaction mixture was concentrated under reduced pressure and the content cooled down in a water and ice bath until precipitates were formed. The mixture was vacuum filtered whilst washing with ethyl acetate producing, **GMPVII**. (76 g, 53.0%). ^{1}H NMR (300 MHz, MeOH-d_4); δ 8.04 (1H, d, J = 3 Hz); 7.83 (2H, dd, J = 9 Hz); 4.85 (3H, s); 4.50 (2H, t, J = 9.0 Hz); 3.30 (1H, q, J = 3.0 Hz); 1.95 (2H, q, J = 3.0 Hz); 1.62 (6H, s); 1.28 (18H, m); 0.89 (3H, t, J = 6.0 Hz). ^{13}C NMR (75 MHz, MeOH-d_4); δ 144.09, 140.28, 132.25, 126.88, 123.83, 116.94, 54.71, 48.39, 47.61, 31.66, 29.32, 29.21, 29.08, 29.05, 28.83, 27.45, 26.28, 22.33, 21.29, 13.07.

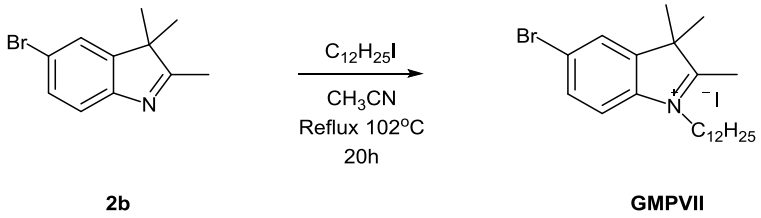

2,3,3-trimethyl-3H-indole (5b): **4b** (2.50 g, 23.1 mmol)) and 3- methyl-2-butanone (4.00 g, 46.2 mmol) were refluxed in ethanol (25 mL) under a nitrogen-filled atmosphere for 30 minutes. Ethanol was evaporated under reduced pressure, acetic acid (25 mL) was added to the reaction mixture and the content refluxed for 4 hours. The reaction mixture was poured over a saturated sodium bicarbonate solution (100 mL) and the organic layer

extracted by dichloromethane (85 mL). Lastly, the solvent was evaporated producing a light red/yellow oil which was used in the next step without further purification, **5b** (3.42 g, 92 %).

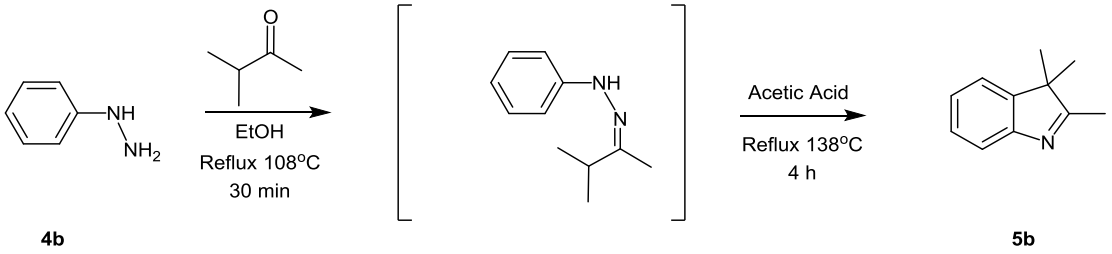

4b **5b**

1-ethyl-2,3,3-trimethyl-3H-indol-1-ium (6b): **5b** (3.42 g, 21.4 mmol) and 1-iodoethane (6.70 g, 42.9 mmol), were dissolved in acetonitrile (15 mL) and refluxed under a nitrogen atmosphere overnight. The reaction was stopped and slowly cooled to room temperature, inducing crystallization of a solid within the reaction mixture. Vacuum filtration followed isolating the solid, **6b**. (5.12 g, 76%). ^{1}H NMR (300 MHz, $CDCl_3$); δ 7.72 (1H, dd, J = 3.0 Hz); 7.56 (3H, m); 4.71 (2H, q, J = 6.0 Hz); 3.11 (3H, s); 1.62 (6H, s); 1.59 (3H, t, J = 12.0 Hz). ^{13}C NMR (75 MHz, $CDCl_3$); δ 195.36, 141.66, 140.54, 130.15, 129.57, 123.42, 115.34, 54.45, 45.65, 23.10, 16.99, 13.62.

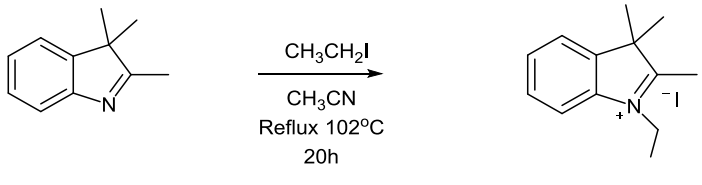

5b **6b**

1-ethyl-3,3-dimethyl-2-methyleneindoline (7b): **6b** (2.00 g, 6.3 mmol) was introduced to a 1M aqueous sodium hydroxide solution (5.08 g, 124 mmol), after which toluene (127 mL) was added under vigorous mixing for 1 hour. Reaction mixture was then extracted using dichloromethane (30 mL) and the solvent evaporated under reduced

pressure producing the desired product, **7b** (1.20 g, quantitative) which was then used without further purification.

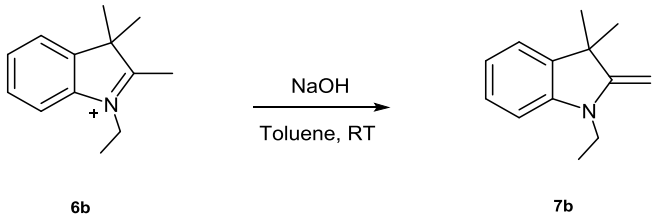

6b 7b

(E)-3-ethoxy-4-((1-ethyl-3,3-dimethylindolin-2-ylidene)methyl)cyclobut-3-ene-1,2-dione (8b): **7b** (1.20 g, 6.4 mmol), 3,4-diethoxycyclobut-3-ene-1,2-dione (1.10 g, 6.4 mmol), and triethyl amine (0.65 g, 6.4 mmol) were dissolved in ethanol (100 mL) and refluxed overnight under a nitrogen atmosphere. The solvent was evaporated under reduced pressure leaving a dark green viscous liquid which was purified by column chromatography (Silica gel; using dichloromethane as an eluent) to collect the product **8b** as a dark red solid (0.91 g, 45%). ^{1}H NMR (400 MHz, $CDCl_3$) δ 7.28 (4H, m); 5.40 (1H, s); 4.90 (2H, q, J = 3.0 Hz); 3.89 (2H, q, J = 9.0 Hz); 1.62 (6H, s); 1.53 (3H, t, J = 9.0 Hz).

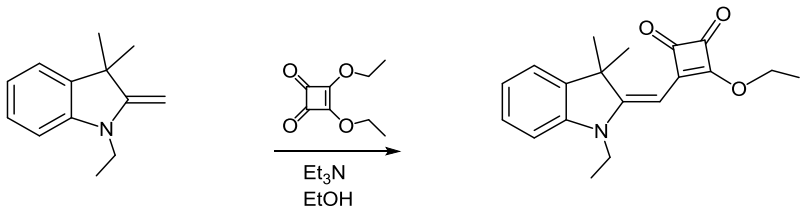

7b 8b

(E)-3-((1-ethyl-3,3-dimethylindolin-2-ylidene)methyl)-4-hydroxycyclobut-3-ene-1,2-dione (GMPVIII): **8b** (0.91 g, 2.9 mmol) was dissolved in ethanol (20 mL) and refluxed for 30 minutes. An aqueous solution of sodium hydroxide (1.17 g, 29.2 mmol) was then added and the mixture was refluxed for 30 minutes. The reaction mixture was cooled and

hydrochloric acid (7% by weight) was added drop wise until a pH of 3 was achieved. Ethanol was removed under reduced vacuum and the reaction mixture extracted with dichloromethane (80 mL). The product was dried using sodium sulfate to yield **GMPVIII** (0.60 g, 73%) which was used in the next step without further purification.

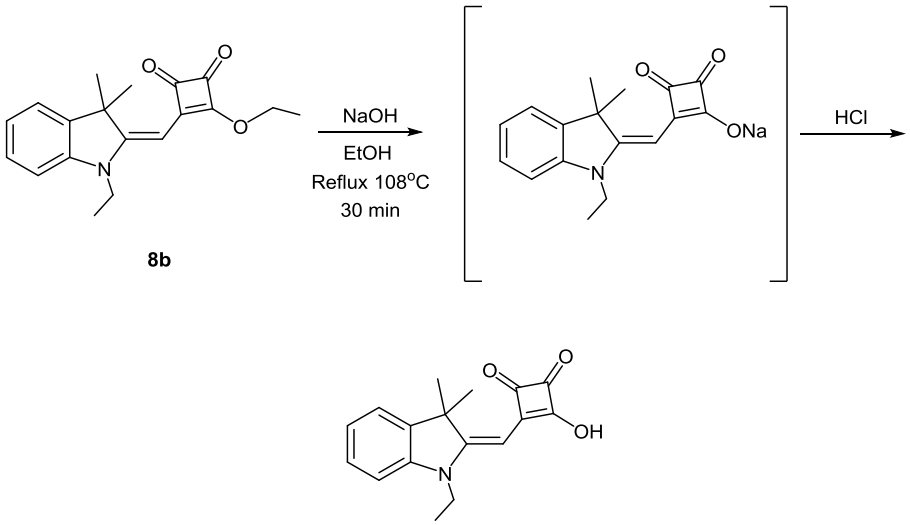

(E)-2-((Z)-(5-bromo-1-dodecyl-3,3-dimethylindolin-2-ylidene)methyl)-4-((1-ethyl-3,3-dimethyl-3H-indol-1-ium-2-yl)methylene)-3-oxocyclobut-1-enolate (GMPIX):

GMPVIII (0.60 g, 2.1 mmol) was dissolved in dry toluene (20 mL) with sonication and was introduced into a solution of **GMPVII**(1.13 g, 2.1 mmol) in dry butanol (9 mL). The reaction mixture was refluxed and water was removed via a Dean-Stark trap filled with dry toluene (10 mL) overnight. The dark blue reaction mixture was then purified via column chromatography (Silica gel; using dichloromethane first to rid of impurities and then slowly increasing the polarity of the eluent by gradually adding ethyl acetate until the compound was isolated with 25% ethyl acetate in dichloromethane). to get the desired product **GMPIX** (1.00 g, 76%). ^{1}H NMR (300 MHz, $CDCl_3$); δ 7.35 (7H, m); 5.98 (2H, s); 4.10 (3H, q, J = 6.0 Hz); 1.78 (12H, s); 1.40 (3H, t, J = 6.0 Hz); 1.24 (21H, m); 0.87

(3H, t, J = 6.0 Hz). ^{13}C NMR (300 MHz, $CDCl_3$); δ 182.19, 180.70, 178.57, 170.41, 168.38, 142.24, 141.71, 130.53, 128.93, 128.12, 127.83, 125.52, 125.21, 124.02, 122.30, 116.04, 110.04, 109.37, 86.74, 86.51, 60.29, 49.45, 49.02, 43.65, 31.83, 29.51, 29.44, 29.40, 29.29, 29.25, 27.07, 26.96, 26.81, 22.62, 14.10, 12.03.

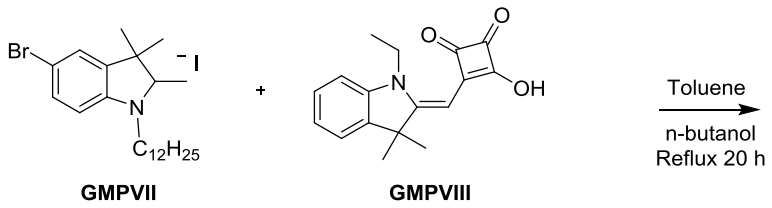

GMPVII **GMPVIII**

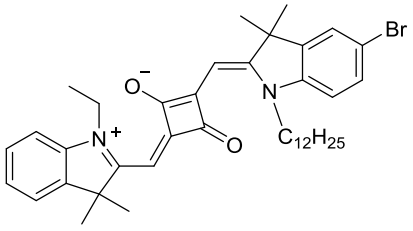

GMPIX

Synthesis of a Thiophene Bridge with a Perfluorinated Alkyl Chain

Synthesis of **GMPII** was initially attempted following **Scheme 2**. Due to time constraints only some of the steps towards **GMPII**'s complete synthesis were accomplished as shown in **Scheme 3**.

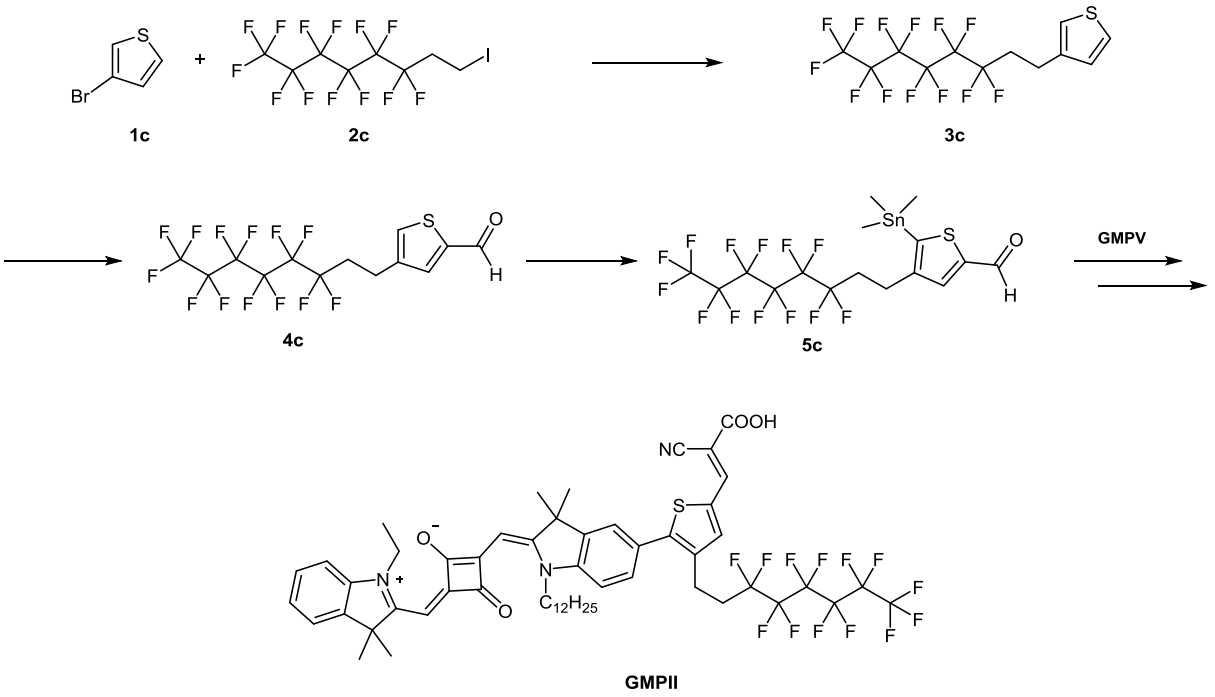

Scheme 2. Overview of the synthetic route taken to produce the desired asymmetrical squaraine dye with the perfluorated alkyl chain.

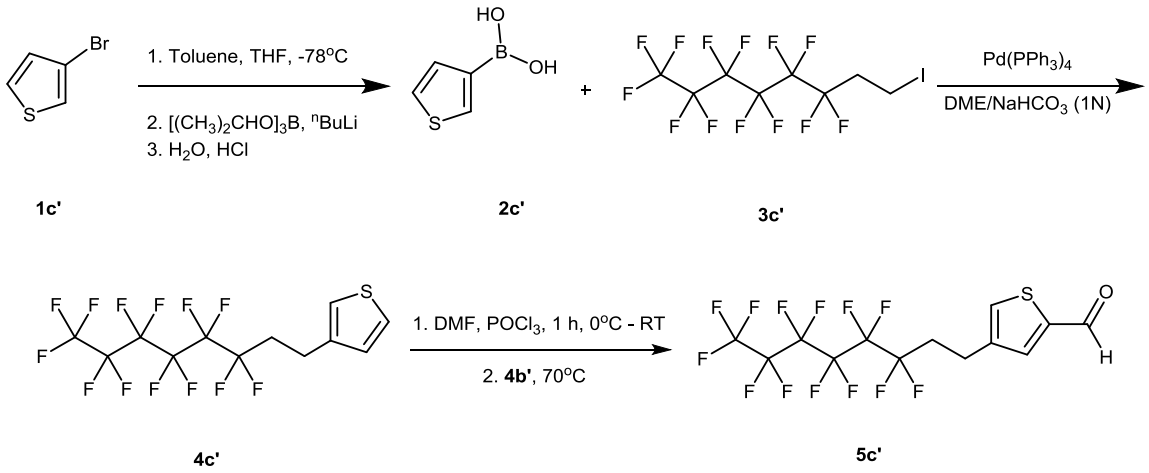

Scheme 3. Alternate pathway for the synthesis of **GMPII**.

Thiophen-3-ylboronic acid (2c'): A dry, three-necked round bottom flask was placed under a nitrogen atmosphere and to it **1c'** (5.0 g, 30.7 mmol), THF (15 mL), toluene (47 mL) and tri-isopropyl borate (6.9 mmol, 36.8 mmol) were added. After cooling the mixture to -78 ^{o}C, n-butyllithium (16 mL, 36.8 mmol) was introduced dropwise. Reaction was warmed to room temperature overnight. Water (100 mL) was added and stirred for 2 hours. Addition of hydrochloric acid HCl (~5 mL, 35% in water) followed in order to reach a pH of 1, later extracting with DCM (35 mL) and concentrating to yield a white solid. The solid was recrystallized from hexanes to get **2c'** (1.88 g, 47%). ^{1}H NMR (300 MHz, Acetone-d_6) δ 7.99 (1H, m); 7.48 (1H, m); 7.43 (1H, m), 7.16 (2H, m).

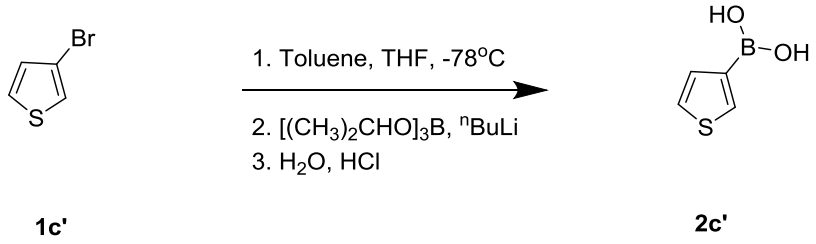

3-(3,3,4,4,5,5,6,6,7,7,8,8,8-tridecafluorooctyl)thiophene (4c'): 2c' (0.88 g, 6.9 mmol) and tetrakis triphenyl phosphine palladium (0.20 g, 0.2 mmol) were introduced into a dry,

three-necked round bottom flask under a nitrogen atmosphere. Dimethoxyethane (DME) (40 mL), 1,1,1,2,2,3,3,4,4,5,5,6,6-tridecafluoro-8-iodooctane (**3c'**) (3.62 g, 7.5 mmol), and sodium bicarbonate solution in water (20 mL, 1N) were added together and the reaction mixture was set to reflux for 5 hours. The reaction was stopped, cooled down, and the organic layer was extracted with diethyl ether (3 x 10 mL) and the combined extracts were washed with brine solution (3 x 10 mL). Evaporation of the organic phase yielded a dark viscous fluid. The product was purified chromatographically (silica gel and ligroin as the eluent) to get the product as a waxy solid **4c'** (0.50 g, 17%). ^{1}H NMR (300 MHz, $CDCl_3$) δ 7.90 (1H, m); 7.59 (1H, m); 7.45 (1H, m), 2.07 (2H, t, J = 3.0), 1.92 (2H, m).

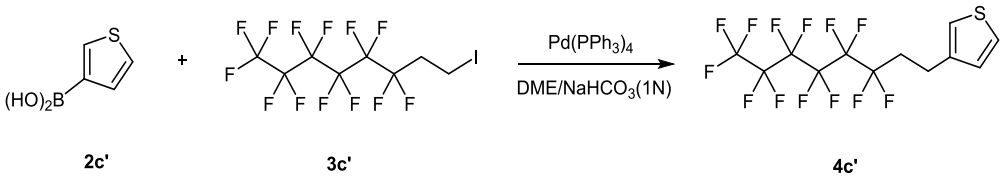

2c' 3c' 4c'

4-(3,3,4,4,5,5,6,6,7,7,8,8,8-tridecafluorooctyl)thiophene-2-carbaldehyde (5c'): A microwave tube was sealed under nitrogen. *N*,*N*-dimethylformamide (0.07 mL), and phosphorus oxychloride (0.17 g, 1.12 mmol) were added and content cooled to 0 ^{o}C before addition of **4c'** (0.40 g, 0.93 mmol) dissolved in 0.5 mL of *N*,*N*-dimethylformamide. The reaction mixture was left to proceed over the weekend at 70 ^{o}C. Purification of the reaction mixture followed via a silica gel column packed with ligroin and using 1:1 DCM and ligroin mixture as eluent to yield **5c'** (21 mg, 5.0%). ^{1}H NMR (300 Hz, $CDCl_3$); δ 11.10 (1H, s); 7.42 (1H, m); 7.18 (1H, m); 2.33 (2H, t, J = 3.0 Hz); 1.99 (2H, m).

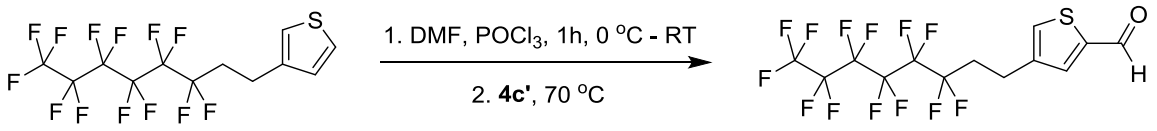

4c' **5c'**

Synthesis of the fluorinated alkyl chains proved to be nontrivial. The synthesis was not completed, bridge compound was not able to be synthesized during the duration of this project; however, a clear idea of a procedure leading up to the production of the aldehyde product was established. This will be helpful for future scale up reactions that will lead to the full synthesis of the modified squaraine dye.

CHAPTER 3

OPTOELECTRONIC PROPERTIES AND EFFECTS OF AGGREGATION

Using the synthesized squaraine bromide as the donor for eight D-π-A systems, optoelectronic properties were measured and effects of aggregation on the dyes were observed. Modification of the π-bridges were an important variable since the push-pull effect of the D-π-A systems relies on the bridge to transfer the charge from the excited donor, in this case the squaraine, to the acceptor anchoring group. The optoelectronic properties measured include the wavelength at which the absorption is the max (λ_{max}), molar extinction coefficient ($\varepsilon[M^{-1}cm^{-1}]$), oscillator strength values (*f*), optical gap ($E_{0\text{-}0}^{opt}$ [eV]), ground state oxidation potential $E_{(S+/S)}$ [V] , and excited state oxidation potential $E_{(S+/S^*)}$ [V] which are shown in the **Table 1** below.

Table 1. Optical properties and electrochemical properties of the synthesized dyes.[a]

Dyes	**λ_{max} [nm]**	**$\varepsilon[M^{-1}cm^{-1}]$**	***f***	**$E_{0\text{-}0}^{opt}$ [eV]**	**$E_{(S+/S)}$ [V]**	**$E_{(S+/S^*)}$ [V]**
YR6	659	279,000	1.39	1.76	0.80	−0.96
T-PA	655	311,000	1.49	1.85	0.86	−0.99
TS3	670	160,000	1.34	1.74	0.74	−1.00
DTP-PA	670	204,000	1.43	1.82	0.82	−1.00
DTT-CA	662	231,000	1.28	1.76	0.80	−0.99
DTT-PA	661	259,000	1.43	1.84	0.85	−0.99
DTS-CA	667	257,000	1.58	1.82	0.84	−0.98
DTS-PA	666	214,000	1.32	1.83	0.88	−0.95

[a]λ_{max} and εwere obtained from absorption spectra in ethanol. $E_{0\text{-}0}^{opt}$ was determined from the intersection of the normalized emission and absorption spectra, while $E_{(S+/S)}$ was obtained via cyclic voltammetry.

From the data it was noted that the DTP, DTS, and DTT dyes with CA end groups appeared to show minute bathochromic shifts with respect to λ_{max} when compared to the simple T bridge, with the largest shift noted being 11 nm as shown in **Figure 8**. Furthermore, having a conjugated bridge introduced significantly higher energy bands between 400 and 550 nm, varying from the nature of the bridge. The molar extinction coefficients ranged from as high as 42,000 $M^{-1}cm^{-1}$ for TS3 with DTP to as low as 26,000 $M^{-1}cm^{-1}$ for YR6 with the T bridge. The integrated area under the absorption peaks was therefore noted to be higher or similar to the dye having the T bridge, as seen in the oscillator strength values *f* in **Table 1**. Concerning the squaraine absorption band, whether a dye had CA or PA groups attached had little effect, but the effects seen on higher energy bands was more noticeable, as seen by the 22 nm hypsochromic shift of the DTP bridge.

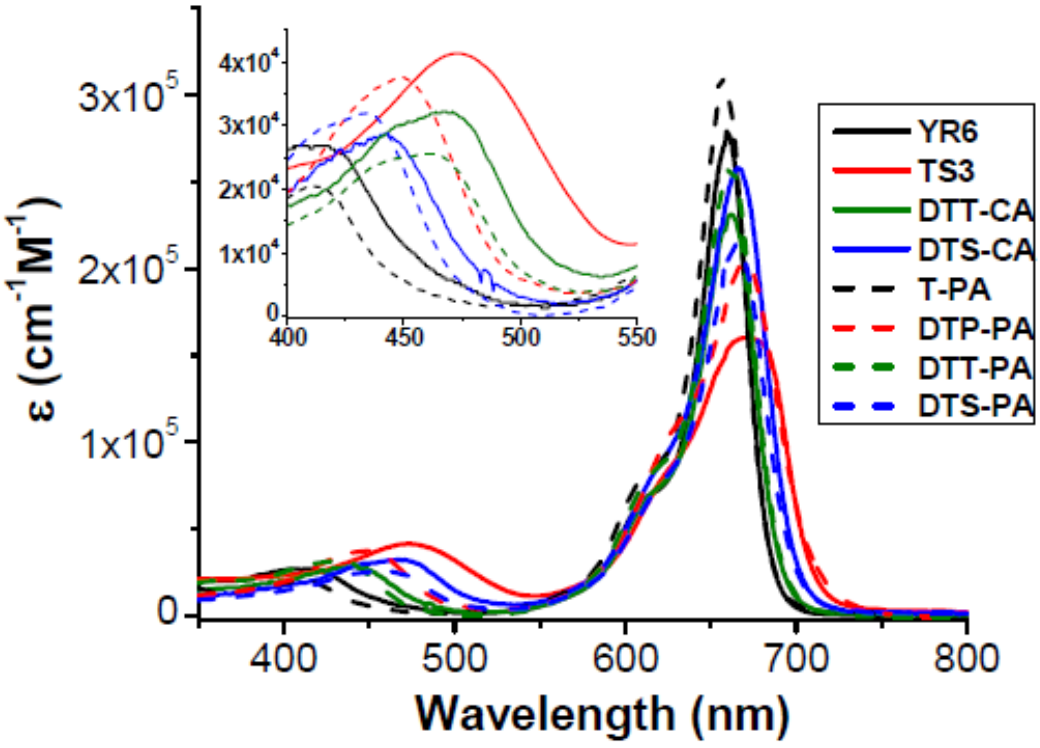

Figure. 8. UV-vis absorption spectra of YR6, TS3, and CA and PA dyes series measured in the solvent ethanol. Axis labels for inset are the same as the larger figure represented.

When measuring electrochemical properties of the dyes it was important to pay close attention to the ground-state oxidation potential ($E_{S+/S}$) and the excited-state oxidation potential ($E_{S+/S*}$) with respect to the electrochemical potential of the electrolyte and the conduction band edge (CBE) of TiO_2. Sufficient driving force is needed for charge injection from the excited dye into the TiO_2 CBE along with the regeneration of the dye via triiodide/iodide redox couple, thus allowing for efficient cycling of charge in squaraine based solar cells. Determining the extent of the driving force is the energy difference between $E_{S+/S*}$ and the TiO_2 CBE (-0.5V vs. NHE) [19,20] which must be at least 150 meV[21] for useful charge transfer. Concerning dye regeneration by the I_3^-/I^- redox couple (0.35 V vs NHE),[22] efficient regeneration can be insured by a $E_{S+/S}$ higher than

0.65 V vs NHE.[22] Reaching above and beyond the minimum required driving force for charge injection into TiO_2 of 450 mV, all of the dyes exhibited driving forces indicating a thermodynamically stable charge injection as shown by the values in **Table 2**. Also seen was the more than sufficient dye regeneration voltages ranging from 0.74 V to 0.88 V vs. NHE for all dyes.

Table 2. Charge injection dynamics of YR6, TS3, and other CA and PA series. The assembled dye cells were pumped near the ground state absorption for each dye and probed near their excited state absorption maxima. All data were fit with stretched exponentials.

Dye	τ_{obs}[ps]/ $_{TiO2}$	τ_{obs}[ps]/ $_{Al2O3}$	K_{ei} [10^{-10} s^{-1}]	ΔG_{ei}^0[V]	ΔG_{reg}^0[V]	η[%]
YR6	1.8	123.9	52.4	0.46	0.50	98.5
T-PA	8.3	80.3	10.8	0.49	0.56	89.6
TS3	1.0	14.1	97.6	0.50	0.44	97.6
DTP-PA	16.0	127.3	5.5	0.50	0.52	87.4
DTT-CA	19.8	3942	5.0	0.49	0.50	99.0
DTT-PA	19.1	32.3	2.2	0.49	0.55	41.0
DTS-CA	1.2	22.6	78.9	0.48	0.54	94.6
DTS-PA	4.0	18.5	19.6	0.43	0.58	78.6

Effects of aggregation on the efficiency of the squaraine-based solar cells we evaluated optically by measurement of their absorption spectra on TiO_2 films as shown in **Figure 9**.

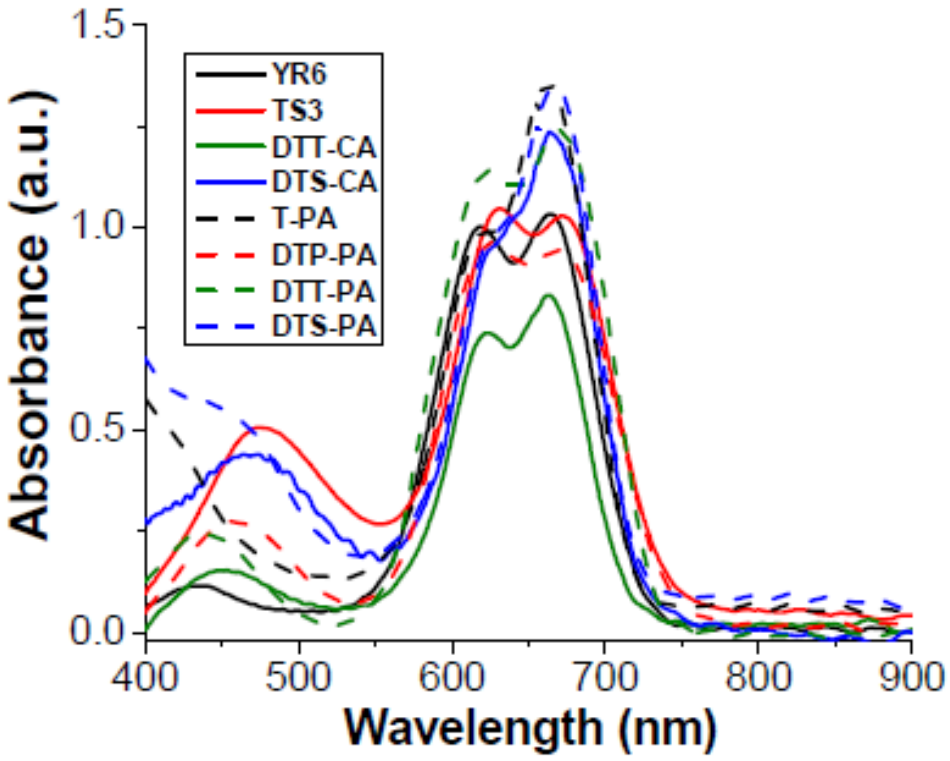

Figure. 9. UV-vis absorption spectra of dyes YR6, TS3 and the other CA and PA dyes after application to TiO_2 films with 0.05 mM dye (0.1 mM for TS3) and 10 mM CDCA after 1 hour of soaking.

The TiO_2 films were immersed into a dye solution dissolved in ethanol and chloroform (4:1) containing 3α,7α-dihydroxy-5β-cholic acid (chenodeoxycholic acid (CDCA) for 12 hours at room temperature. UV-Vis absorption spectra were collected after TiO_2 films were washed with ethanol and dried under N_2. The spectra revealed not only general broadening of peaks for dyes on the film, but also blue-shifted peaks from the main squaraine absorption band were noted. It has been noted in the literature that these peaks have been observed for squaraine dyes when H-aggregation is present.[23, 24] As expected, all the dyes with the exception of DTS-CA and DTS-PA exhibited a well-defined peak associated with H-aggregation. For the DTS dyes, only a shoulder is seen due to the 2-ethylhexyl chains on the bridge projection out of the plane of the squaraine dye and

therefore contributing to the reduction of pi-pi stacking and aggregation. Other dyes were affected majorly by pi-pi stacking due to their planarity as seen by the sharp peak at 630 nm.

The effects of dye aggregation on the performance of assembled cells including the triiodine/iodine electrolyte were explored. CDCA was been shown to increase the PCE of devices, which indicates that aggregation is present within all dyes.[25, 26] Yet, it was noticed that the synthesized dyes with the PA anchoring groups demonstrated a greater dependence on the CDCA:dye ratio when compared to their CA analogs. CDCA has been used extensively in the assembly of solar cells for decreasing aggregation due to its amphiphilic properties and therefore formation of elongated micelles in aqueous media.[27] Hydrogen bonded cluster formation is a reality when producing dyes incorporating hydroxyl groups and phosphonic acids; as a result, further aggregation can result in PA dyes which become increasingly difficult to disaggregate when compared to their CA analogs. This could potentially reduce the disaggregating efficacy of CDCA when assembling dye sensitized solar cells with PA anchoring group dyes.

CHAPTER 4

MEASUREMENTS OF PHOTOVOLTAICS

In order to evaluate the photovoltaic properties of each dye incorporated into a completed cell, the optimized CDCA:dye ratios were determined and the V_{oc} [V], J_{sc} [mA/cm^2], FF [%], and PCE [%] measured as shown in **Table 3** and **Figure 9**. These measurements were based on the data of 3 devices for all dyes with the exception of TS3 with the standard deviation shown. The photovoltaic measurements were conducted in the absence of a mask with a cell active area of 0.36 cm^2, when a mask was utilized a decrease of up to 10% in PCE was observed. TS3 and DTT-CA had measured J_{sc} and V_{oc} values which were consistent with those published in literature.[9, 14, 28] The observed low V_{oc} values were expected since this is a common trend within squaraine sensitizers,

Table 3. Measurements of photovoltaics using optimized CDCA:dye ratios for 4 hours: YR6 (0.1 mM), T-PA (0.05 mM), TS3 (0.1 mM), DTP-PA (0.05 mM), DTT-CA (0.1 mM), DTT-PA(0.1 mM, 50 mM CDCA), DTS-CA (0.05 mM), DTS-PA (0.05 mM).

	***Voc* [V]**	**J_{SC} [mA/cm^2]**	**FF[%]**	**PCE [%]**
YR6	0.647±0.006	14.2±0.3	70.4±0.2	6.5±0.1
T-PA	0.644±0.000	9.6±0.3	72.2±0.6	4.6±0.2
TS3	0.61	13.5	68.3	5.6
DTP-PA	0.642±0.002	5.9±0.4	73.5±0.1	2.8±0.3
DTT-CA	0.644±0.004	13.1±0.3	71.6±1.1	6.0±0.1
DTT-PA	0.621±0.002	3.7±0.2	76.3±0.2	1.8±0.1
DTS-CA	0.682±0.000	19.1±0.2	68.3±0.7	8.9±0.2
DTS-PA	0.676±0.002	10.4±0.2	70.5±0.4	5.0±0.1

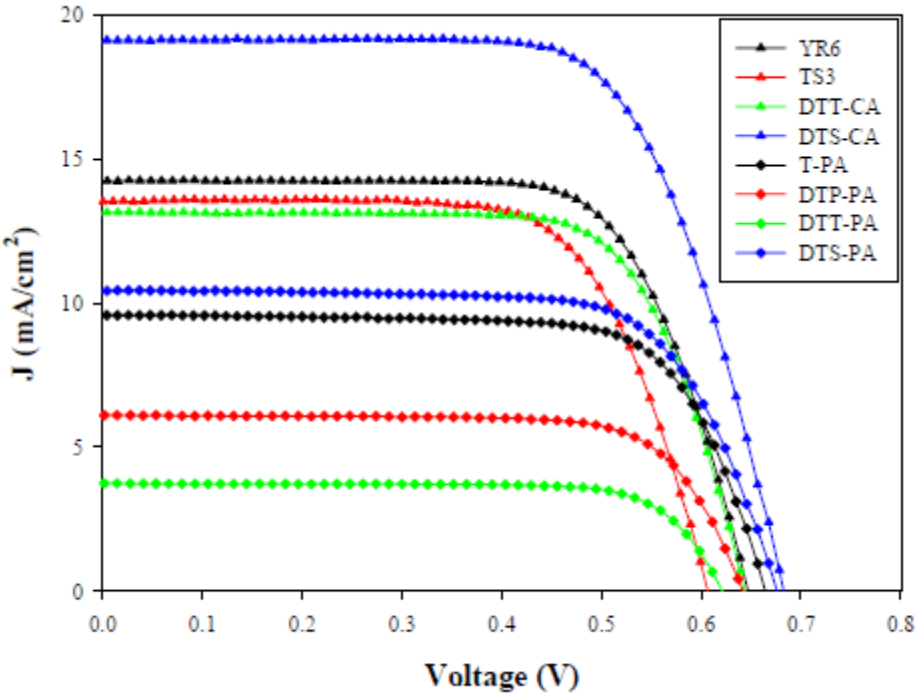

Figure. 10. Measured photovoltaic performance of the selected optimized dye cells with TiO_2 films soaked in dye bath with 10 mM CDCA and different concentration of dye for 4 hours.

limiting their performance despite their relatively high J_{sc}, reaching as high as 16.4 mA/cm^2 as seen in JD10.[14] Concerning DTS-CA, an observed increase in V_{oc} was noted, the highest for a squaraine-based cell at 682 mV, a 47 mV increase over JD10. Again, we believe decreased aggregation from the out-of-plane groups within DTS-CA played an integral part in the increased J_{sc}.

Compared to the CA dyes synthesized, the PA dyes showed significantly lower PCEs, which we believe was due to the lower J_{sc} values observed. This dropped the PCE by up to 72% as seen in the difference between DTT-CA and DTT-PA. Shown in **Figure 11** are the IPCE action spectra, measured in order to gain insight into the J_{sc} values of the DSSCs. Onsets for most CA dyes were seen at around 800 nm with the exception of DTS-CA at 850 nm. Furthermore, DTS-CA showed the highest IPCE measurement when

compared to the other dyes synthesized, 90% at low energies and 83% at higher energies. PA dyes however, showed increasingly narrow features and overall lower IPCEs with maximums at close to 60%. The continuing trend of the drop in the J_{sc} and PCEs helped in explaining the lower IPCE measured when going from CA to PA anchoring groups.

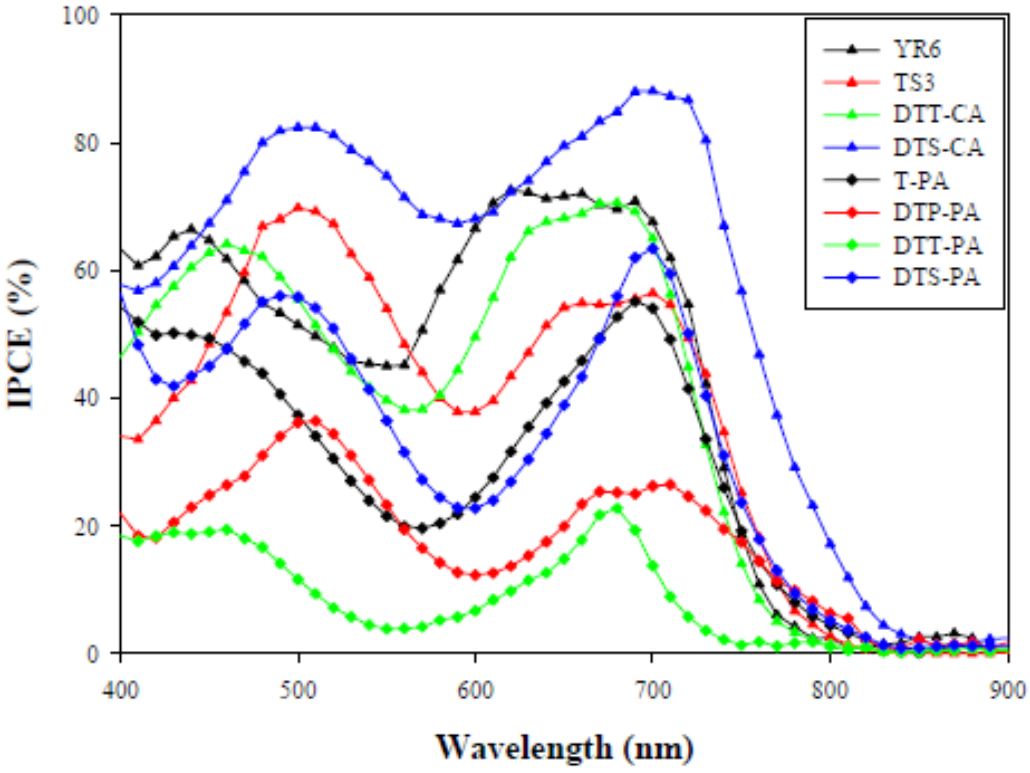

Figure. 11. Measured IPCE of the optimized dye cells with TiO_2 films being soaked in dye bath with the same dye/CDCA ratio in Table 3.

CHAPTER 5

CONCLUSION

During the course of my research experience in the lab of Dr. Seth Marder I was able to immerse myself in different approaches towards tackling relevant and complex problems pertaining to squaraine-based sensitized solar cells. Focusing on the issue of dye aggregation due to π-π stacking, two different approaches were initially tried, both unfortunately ending before complete synthesis of the proposed compounds. These experiences served to educate me first hand in the diverse landscape of reactions, methods, and train of thought utilized in the field of organic chemistry.

Completion of the asymmetrical squaraine, however, led into the synthesis of multiple compounds used by PhD candidate, Fadi Jradi, in order to further study the effects of π-bridges and anchoring groups on solar cell performance as discussed in chapters three and four of this thesis. Overall, dyes with DTS bridges had the highest measured efficiencies within their respective series at 8.9% for the CA anchoring group dyes and 5.0% for those dyes with the PA anchoring. These properties were attributed to the higher J_{sc} and V_{oc} from the decreased dye aggregation and slower recombination rates, respectively. The study suggests dye aggregation can be potentially decreased by incorporation of out-of-plane π-bridge groups with respect to the planar squaraine molecule used. This was seen in the increased J_{sc} and subsequently in the increased PCE.

Future outlook concerning the design of squaraine dyes must focus on increasing the V_{oc}. This value continues to lag behind other state of the art dyes (~ 0.9-1.0 V) such as porphyrins.[18] One approach towards increasing V_{oc} would be to design squaraine dyes

that are compatible with iodine-free electrolytes such as cobalt, and electrolyte known to increase solar cell V_{oc}.

REFERENCES

(1) Hagfeldt, A.; Boschloo, G.; Sun, L.; Kloo, L.; Pettersson, H. *Chem. Rev. (Washington, DC, U. S.)* **2010**, *110*, 6595.

(2) Becquerel, A. E. *C. R. Acad. Sci.* **1839**, *9*.

(3) Schiermeier, Q.; Tollefson, J.; Scully, T.; Witze, A.; Morton, O. *Nature News* **2008**, *454*, 816.

(4) Goetzberger, A.; Luther, J.; Willeke, G. *Sol. Energy Mater. Sol. Cells* **2002**, *74*, 1.

(5) Chapin, D.; Fuller, C.; Pearson, G. *J. Appl. Phys.* **1954**, 676.

(6) Hamann, T. W.; Jensen, R. A.; Martinson, A. B.; Van Ryswyk, H.; Hupp, J. T. *Energy Environ. Sci.* **2008**, *1*, 66.

(7) Nazeeruddin, M. K.; Kay, A.; Rodicio, I.; Humphry-Baker, R.; Müller, E.; Liska, P.; Vlachopoulos, N.; Grätzel, M. *J. Am. Chem. Soc.* **1993**, *115*, 6382.

(8) Mathew, S.; Yella, A.; Gao, P.; Humphry-Baker, R.; Curchod, B. F.; Ashari-Astani, N.; Tavernelli, I.; Rothlisberger, U.; Nazeeruddin, M. K.; Grätzel, M. *Nature Chem.* **2014**, *6*, 242.

(9) Shi, Y.; Hill, R. B. M.; Yum, J.-H.; Dualeh, A.; Barlow, S.; Grätzel, M.; Marder, S. R.; Nazeeruddin, M. K. *Angew. Chem., Int. Ed.* **2011**, *50*, 6619.

(10) Schiffmann, F.; VandeVondele, J.; Hutter, J.; Urakawa, A.; Wirz, R.; Baiker, A. *PNAS* **2010**, *107*, 4830.

(11) O'Regan, B. C.; Walley, K.; Juozapavicius, M.; Anderson, A.; Matar, F.; Ghaddar, T.; Zakeeruddin, S. M.; Klein, C.; Durrant, J. R. *J. Am. Chem. Soc.* **2009**, *131*, 3541.

(12) O'Regan, B. C.; López-Duarte, I.; Martínez-Díaz, M. V.; Forneli, A.; Albero, J.; Morandeira, A.; Palomares, E.; Torres, T.; Durrant, J. R. *J. Am. Chem. Soc.* **2008**, *130*, 2906.

(13) O'Regan, B.; Gratzel, M. *Nature* **1991**, *353*.

(14) Delcamp, J. H.; Shi, Y.; Yum, J. H.; Sajoto, T.; Dell'Orto, E.; Barlow, S.; Nazeeruddin, M. K.; Marder, S. R.; Grätzel, M. *Chem.--Eur. J.* **2013**, *19*, 1819.

(15) Jradi, F. M.; Kang, X.; O'Neil, D.; Pajares, G.; Getmanenko, Y. A.; Szymanski, P.; Parker, T.; El-Sayed, M. A.; Marder, S. R. *Chem. Mater.* **2015**.

(16) Brennan, B. J.; Portolés, M. J. L.; Liddell, P. A.; Moore, T. A.; Moore, A. L.; Gust, D. *Phys. Chem. Chem. Phys.* **2013**, *15*, 16605.

(17) Wiberg, J.; Marinado, T.; Hagberg, D. P.; Sun, L.; Hagfeldt, A.; Albinsson, B. *J. Phys. Chem. C* **2009**, *113*, 3881.

(18) Murakami, T. N.; Yoshida, E.; Koumura, N. *Electrochim. Acta* **2014**, *131*, 174.

(19) Hagfeldt, A.; Graetzel, M. *Chem. Rev. (Washington, DC, U. S.)* **1995**, *95*, 49.

(20) Kalyanasundaram, K.; Grätzel, M. *Coord. Chem. Rev.* **1998**, *177*, 347.

(21) de Miguel, G.; Marchena, M.; Cohen, B.; Pandey, S.; Hayase, S.; Douhal, A. *J. Phys. Chem. C* **2012**, *116*, 22157.

(22) Boschloo, G.; Hagfeldt, A. *Acc. Chem. Res.* **2009**, *42*, 1819.

(23) de Miguel, G.; Marchena, M.; Ziółek, M.; Pandey, S.; Hayase, S.; Douhal, A. *J. Phys. Chem. C* **2012**, *116*, 12137.

(24) de Miguel, G.; Ziółek, M.; Zitnan, M.; Organero, J.; Pandey, S.; Hayase, S.; Douhal, A. *J. Phys. Chem. C* **2012**, *116*, 9379.
(25) Herndon, W. C. *J. Chem. Educ.* **1967**, *44*, 724.
(26) Chen, M.; Gratzel, M.; Thomas, J. *J. Am. Chem. Soc.* **1975**, *97*, 2052.
(27) Kay, A.; Graetzel, M. *J. Phys. Chem.* **1993**, *97*, 6272.
(28) Mulhern, K. R.; Orchard, A.; Watson, D. F.; Detty, M. R. *Langmuir* **2012**, *28*, 7071.